Am J Transl Res 2017;9(3):1369-1380
www.ajtr.org /ISSN:1943-8141/AJTR0041166

*Original Article*

# B7-H3 regulates migration and invasion in salivary gland adenoid cystic carcinoma via the JAK2/STAT3 signaling pathway

Teng-Fei Fan[1*], Wei-Wei Deng[1*], Lin-Lin Bu[1], Tian-Fu Wu[1,2], Wen-Feng Zhang[1,2], Zhi-Jun Sun[1,2]

*[1]The State Key Laboratory Breeding Base of Basic Science of Stomatology & Key Laboratory of Oral Biomedicine Ministry of Education, Wuhan University, Wuhan, China; [2]Department of Oral Maxillofacial-Head Neck Oncology, School and Hospital of Stomatology, Wuhan University, Wuhan, China. [*]Equal contributors.*

Received October 4, 2016; Accepted February 9, 2017; Epub March 15, 2017; Published March 30, 2017

**Abstract:** B7 Homolog 3 (B7-H3), a newly identified member of the B7 family, is over-expressed in various human cancers and plays a vital role in tumor progression. To identify the expression pattern of B7-H3 in human salivary adenoid cystic carcinoma (AdCC) and its underlying mechanisms, we characterized B7-H3 expression in AdCC tissue microarrays using immunohistochemical staining, and analyzed potentially associated molecules. The results showed that B7-H3 was highly expressed in salivary AdCC, compared with normal salivary glands. Statistical analyses of immunohistochemical staining showed that B7-H3 was closely correlated with Slug and p-STAT3. Functional studies showed that knockdown of B7-H3 in AdCC cell lines using RNA interference did not influence cell growth and apoptosis, but decreased migration and invasion *in vitro*. Further mechanism studies suggested that B7-H3 influenced the migration and invasion of AdCC cells by regulating the epithelial-mesenchymal transition via JAK2/STAT3 pathway components. Collectively, these findings suggested that B7-H3 may be a potential therapeutic target for AdCC.

**Keywords:** B7-H3, adenoid cystic carcinoma, epithelial-mesenchymal transition, JAK2, STAT3

## Introduction

Adenoid cystic carcinomas (AdCC) are rare variants of adenocarcinoma that most often arise in the salivary glands [1]. Clinical studies indicated that salivary AdCC were characterized by invasive local growth and a high incidence of lung metastasis [2]. Patients with lung metastasis of the salivary AdCC have poor prognoses [3]. However, the precise mechanisms underlying invasion and metastasis in AdCC are not known. Therefore, there is an urgent need to develop new agents and strategies with high efficacy for the treatment of salivary AdCC.

B7 homolog 3 protein (B7-H3), a transmembrane protein with an immunoglobulin-like structure [4], is known to have immunoregulatory properties, with both inhibitory and stimulatory effects on the activation of T cells [5, 6]. As a tumor-associated antigen, B7-H3 is not only involved in tumor immunity, but also plays a non-immunological role in cancer progression. A recent report suggested that overexpression of B7-H3 promoted cutaneous malignant melanoma cell migration and invasion [7]. In addition, the functional knockdown of B7-H3 suppressed the proliferation, colony formation, migration, and invasion in human esophageal cancer [8]. These results strongly suggest that B7-H3 is involved in cancer progression and metastasis.

The epithelial-mesenchymal transition (EMT) process consists of a set of rapid changes in the cellular phenotype during which epithelial cells experience a molecular switch from a polarized, epithelial phenotype to a highly motile, non-polarized mesenchymal phenotype [9, 10]. The EMT is frequently observed at the invasive front of advanced tumors and significantly correlated with metastasis in tumor progression [11-13]. However, whether B7-H3 influ-

ences the EMT in salivary AdCC remains unclear.

In the present study, B7-H3 and EMT molecules expression in salivary AdCC tissue were observed based on serial sections. Tissue microarrays were used to explore the associated molecules. In addition, we determined the function and mechanism of B7-H3 using *in vitro* knockdown assays of B7-H3.

## Materials and methods

### *Cell lines, antibodies and reagent*

Human salivary AdCC cell lines SACC-83 and SACC-LM were obtained from the China Center for Type Culture Collection, and grown in RPMI 1640 medium (Hyclone) containing 10% FBS (fetal bovine serum) [14]. Chemical reagents for experiment were purchased from Sigma-Aldrich (St. Louis, MO), unless otherwise specified. B7-H3 siRNAs were purchased from Sigma-Aldrich with 2 different sequences. Primary antibody against human B7-H3, E-cadherin, N-cadherin, Vimentin, Slug and p-STAT3 were purchased from Cell Signaling Technology (Danvers, MA).

### *B7-H3 siRNA transfection*

To further analyze the role of B7-H3 in AdCC malignancy, human SACC-83 and SACC-LM cell lines were transfected with B7-H3 siRNA using lipofectamine 2000 (Invitrogen, Carlsbad, CA) as previously been described [14]. The sequences of the B7-H3 are 5'-TGAAACACTCTGACAGCAAAGAAGATGA T-3' (siB7-H3-1) and 5'-AGCAC TGTGGTTCTGCCTCACA-3' (siB7-H3-2). The validated non-targeted control (negative control) sequence was 5'-GCACTACCAGAGCTAACTCAGAT AGTACT-3', while mock transfections (Mock) were carried out with lipofectamine 2000 transfection reagent only. After 48 h, transfected cells were harvested for Western blotting analysis.

### *Cell proliferation by MTT assay*

The MTT assay was used to study the effect of B7-H3 RNA interference on AdCC cell viability as previously described [15]. Briefly, cells were suspended at a density of $5 \times 10^3$ cells per well in 200 μl of RPMI 1640 medium in 96-well plates, and continue cultured overnight. The medium was replaced with 100 μl fresh medium containing 0.5 mg/ml MTT (Sigma, USA) at indicated time points. Four hours after the coculture with MTT, the supernatants were removed and discarded. 150 μl of dimethylsulfoxide (DMSO, Sigma) was added to each well to dissolve the crystals. Cell viability was determined by scanning with a microplate reader at a wavelength of 490 nm. Each experiment was performed in triplicate and repeated at least three times.

### *Wound healing assay*

*In vitro* wound healing assay was performed as described previously [16]. Briefly, SACC-83 and SACC-LM cell lines were seeded in 6-well plates (Corning Life Sciences, USA) at $1.0 \times 10^5$ cells/well. When the cells reached 80% confluence, the center of each well was scratched with a sterile pipette tip to generate a constant gap. The cells were continued incubated with serum free medium for additional 24 hours. The cells were photographed under phase microscopy and counted after fixation as previously described [16].

### *Transwell migration assays*

*In vitro* migration assay was performed using 8 μm pore size Transwell® inserts (#3422, Corning, Albany, NY) as described previously [17]. Briefly, $10^4$ cells were placed on the top of the Transwell® chamber inserts. Serum (5%) was used as the chemoattractant. To rule out the effect of cell proliferation, 2 μg $ml^{-1}$ mitomycin C was added to the cells. Cells on the lower surface of the inserts were stained and counted using a light microscope.

### *Cell immunofluorescence*

SACC-83 and SACC-LM cell lines were seeded onto coverslips at a density of $10^5$/mL and cultured in a 6-well plate for 24 hours with the indicated treatment. After treatment, cells were washed twice in PBS and fixed in 4% paraformaldehyde for 30 minutes. Then cells were permeabilized in 0.2% Triton X-100 in PBS for 15 minutes, and blocked by non-immune goat serum for 60 minutes at room temperature. Then cells were incubated with indicated primary antibody at 4°C overnight respectively.

The next day, slides were incubated with fluorochrome conjugated secondary antibodies (PerCP-Cy5.5 anti-rabbit, Jackson ImmunoRe-

search, USA) and mounted in Vectashield with 4', 6-diamidino-2-phenylindole (DAPI; Vector Laboratories). Fluorescence images were then captured using a CLSM-310, Zeiss fluorescence microscope.

*Western blot analysis*

Western blot analysis was performed as previously described [18]. Briefly, SACC-83 and SACC-LM cell lines were transfected with B7-H3 siRNA (100 nM, Sigma-Aldrich), mock, and negative control siRNA. The cells were lysed in a T-PER buffer containing 1% phosphatase inhibitors and complete mini cocktail (Roche) 48 h after transfection. Proteins from each sample were denatured and then loaded in each lane of 12% SEMS polyacrylamide gel electrophoresis. Subsequently, proteins were transferred onto a polyvinylidenefluoride membranes (Millipore, Billerica, MA) and blocked with 5% non-fat milk for 1 hour, then incubated with following primary antibody B7-H3, JAK2, p-JAK2, STAT3, and p-STAT3 at 1:1000 dilution. After overnight incubation at 4°C, membranes were washed for three times and then incubated with second antibody for 1 h at room temperature and visualized with enhanced chemi-luminescence.

*Human salivary AdCC tissue microarray*

The human salivary gland AdCC specimen tissue microarrays used in the present study were obtained from the Department of Oral and Maxillofacial Surgery, School and Hospital of Stomatology Wuhan University (PI: Zhi-Jun Sun) [14]. All patients histologically diagnosed as AdCC by two independent pathologists were included in the present study. The classification of the World Health Organization was used to determine the histologic phynotype. The AdCC cohort consisted of 72 AdCCs (cribriform pattern: 28, tubular pattern 24, solid pattern 20), 12 PMAs and 18 NSGs as previous described [14].

*Immunohistochemistry, digital pathology and scoring system*

The methods and processes of immunohistochemistry were previously reported [19]. Briefly, all AdCC tissue microarrays were cut into 4-μm sections. The slides were deparaffinized and rehydrated. The sections were boiled in 0.01 M citric acid buffer solution (pH 6.0) or 1 mM EDTA buffer solution (pH 8.0) for 1.5 min at high pressure. Subsequently, the samples were incubated with 3% hydrogen superoxide for 20 minutes to quench endogenous peroxidase activity, and 10% goat serum was used to block non-specific binding. The sections were incubated with anti-human B7-H3 (1:200), Slug (1:200), p-STAT3 (1:200). A positive slide was set at each experiment. Subsequently, an avidin-biotin peroxidase reagent was added onto the slides. After washing with phosphate buffer saline, 3,3'-diaminobenzidine tetrachloride was added to the sections, followed by counterstaining with Mayer's hematoxylin.

The immunohistochemical staining was scanned using an Aperio ScanScope CS whole slice scanner (Vista, CA, USA) with background subtraction as previously described [21]. The membrane, nuclear, or pixel immunohistochemical staining was quantified using Aperio Quantification software. The histoscore of the membrane and nuclear staining quantification were assessed according to the formula (3 + percent cells) × 3 + (2 + percent cells) × 2 + (1 + percent cells) × 1, and the formula total intensity/total cell number was used to assess the histoscore of pixel quantification. In this case, the normalized score is between 0 and 300. This method has previously been described [22]. The immunohistochemical staining histoscores were converted to the range of -3 to 3 using Microsoft Excel software as previously described [23]. Cluster 3.0 with average linkage based on Pearson's correlation coefficient was used for hierarchical analysis, and the results were visualized using Java TreeView1.0.5.

*Statistical analysis*

All values are expressed as the means ± SEM. The statistical data analysis was performed using GraphPad Prism 5.03 (GraphPad Software, Inc., La Jolla, CA) statistical package. The differences in immunostaining and protein levels among each group were analyzed by the one-way ANOVA followed by the post-Tukey multiple comparison tests. Student's *t*-test was used for two-group analysis. All experiments were independently repeated in triplicate. $P < 0.05$ was regarded as statistical significance; all tests were two-sided and no correction was

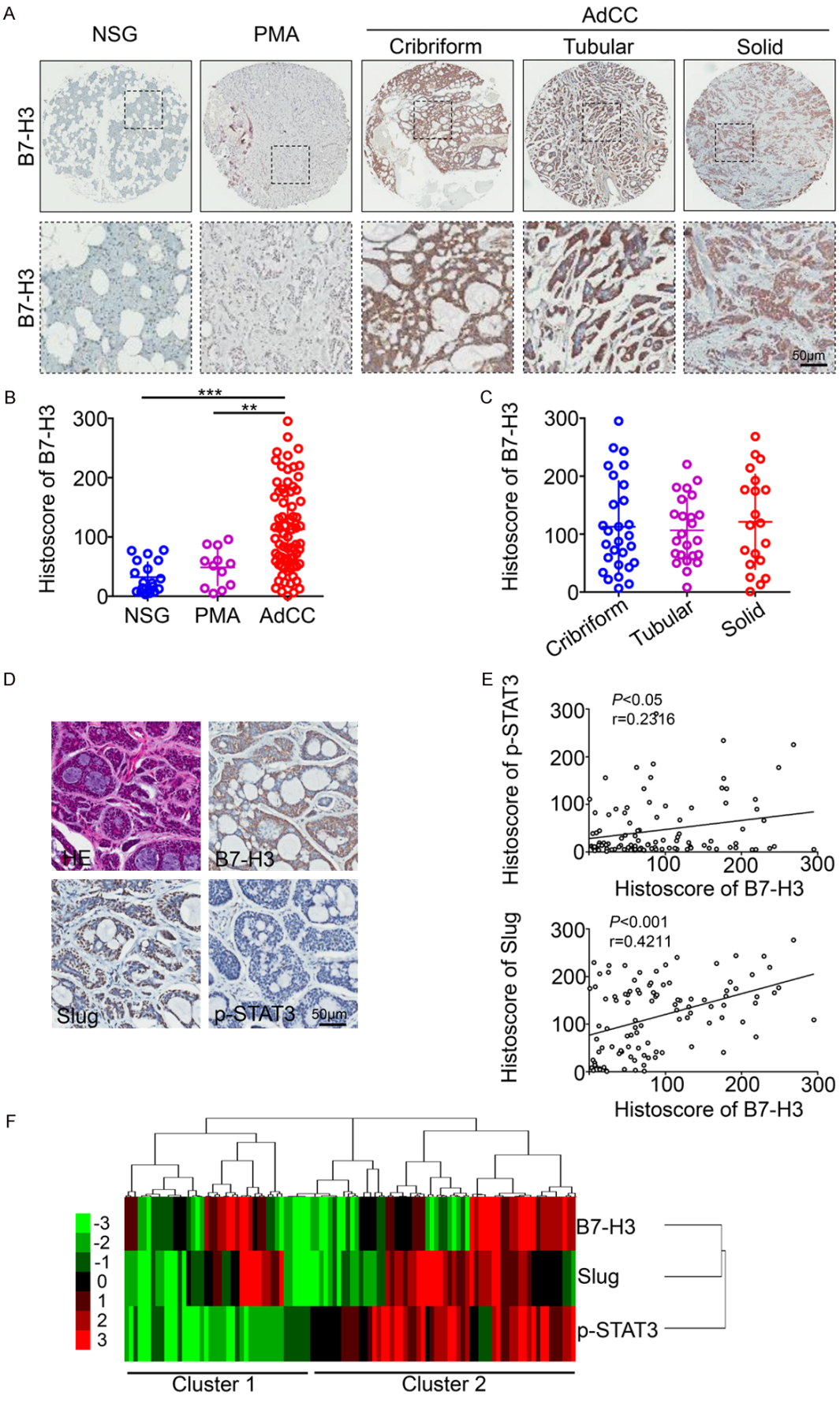
A
NSG
PMA
AdCC
Cribriform
Tubular
Solid
B7-H3
B7-H3
50μm
B
***
**
Histoscore of B7-H3
300
200
100
0
NSG
PMA
AdCC
C
Histoscore of B7-H3
300
200
100
0
Cribriform
Tubular
Solid
D
HE
B7-H3
Slug
p-STAT3
50μm
E
Histoscore of p-STAT3
P<0.05
r=0.2316
Histoscore of B7-H3
Histoscore of Slug
P<0.001
r=0.4211
Histoscore of B7-H3
F
-3
-2
-1
0
1
2
3
B7-H3
Slug
p-STAT3
Cluster 1
Cluster 2

**Figure 1.** B7-H3 immunoreactivity is significantly increased in salivary AdCC, which is correlated with expression of Slug and p-STAT3. A. Representative immunohistochemical staining of B7-H3 in human AdCC tissue (right panel) compared with normal salivary gland (NSG, left panel) and pleomorphic adenoma (PMA, middle panel) (Scale bars = 50 μm); B. Quantification of B7-H3 immunohistochemical expression levels in human NSG, PMA and AdCC tissue as indicated by histoscore (**$P < 0.01$; ***$P < 0.001$, One-way ANOVA with GraphPad Prism 5.0); C. Comparison between different pathological types of B7-H3, expression of B7-H3 was not statistically different between cribriform, tubular and solid type of human salivary AdCC. D. Representative hematoxylin-eosin staining (HE) and immunohistochemical staining of B7-H3, Slug and p-STAT3 in human AdCC tissue (Scale bars = 50 μm); E. B7-H3 was found to be closely associated the Slug ($P < 0.001$, r = 0.4211) and p-STAT3 ($P < 0.05$, r = 0.2316) immunoreactivity. F. Hierarchical clustering presents the protein expression correlation of B7-H3, p-STAT3$^{T705}$, and Slug in human AdCC tissue microarrays.

applied for multiple significance testing. *, **, and *** indicated $P < 0.05$, $P < 0.01$ and $P < 0.001$, respectively.

## Results

### *B7-H3 immunoreactivity was significantly increased and correlated with Slug and p-STAT3 in salivary AdCC*

Immunohistochemistry for B7-H3 was performed on tissue microarrays, including human AdCC (n = 72), common salivary gland benign tumor polymorphic adenoma (PMA, n = 12), and normal salivary glands (NSG, n = 25). The results indicated that B7-H3 immunoreactivity was weakly expressed in NSG and PMA tissues, whereas AdCC showed strong protein expression in the tumor cells, especially at the invasive front (**Figure 1A**). To more precisely determine the difference, we quantified the expression using Aperio ImageScope software, version 12.0 (Leica Biosystems, Buffalo Grove, IL, USA). The results showed that B7-H3 was significantly increased in AdCC compared with PMA ($P < 0.01$) and NSG ($P < 0.001$; **Figure 1B**). However, B7-H3 was not associated with the pathological parameters of different subtypes (cribriform, tubular and solid type) of AdCC (**Figure 1C**). To investigate the possible relation of B7-H3 with EMT marker Slug and p-STAT3, the immunostaining of Slug and p-STAT3 were performed base on serial section of tissue microarrays (**Figure 1D**). Quantification of immunohistochemistry of AdCC and normal oral mucosa tissues indicated by histoscores showed that B7-H3 was statistically associated with p-STAT3 ($P < 0.05$, r = 0.2316; **Figure 1E**) and Slug ($P < 0.001$, r = 0.4211; **Figure 1E**) as assessed by the Spearman's rank correlation coefficient test and the linear regression tendency test. Notably, the expression of B7-H3, p-STAT3, and Slug, in most of the AdCC cases (cluster 2), were distinct from those of the normal mucosa (cluster 1), the hierarchical cluster reflecting the correlation of in B7-H3 with Slug staining in AdCC (**Figure 1F**).

### *Knockdown of B7-H3 showed no effect on AdCC cell proliferation*

To characterize the role of B7-H3 in AdCC, two different siRNAs were designed for knockdown of B7-H3 (**Figure 2A**, **2B**). The knockdown efficiency of B7-H3 was > 70% (**Figure 2A**, **2B**). We then measured the cell proliferation rate *in vitro* using the MTT assay. The results showed that there was no difference in cellular proliferation between the B7-H3 knockdown group and the control group in both the SACC-83 and SACC-LM cell lines (**Figure 2C**, **2D**).

### *Knockdown of B7-H3 by RNA interference decreased AdCC cell migration and invasion*

To further determine the relationship of B7-H3 with cell migration and invasion, we employed wound healing assays to examine the cytological effects of B7-H3 on the migration ability of AdCC cells, and Transwell® invasion assays to determine the key factors involved in malignant progression and metastasis during B7-H3 downregulation. The knockdown of B7-H3 significantly decreased the cell mobility of SACC-83 ($P < 0.01$, **Figure 3A**) and SACC-LM ($P < 0.01$, **Figure 3B**) cells as indicated by *in vitro* wound healing assay 24 hours between the negative control group and the B7-H3 siRNA treatment group. Likewise, the results of the Transwell® assay also showed that knockdown of B7-H3 significantly decreased the transmembrane cell numbers compared with that of the negative control group, in SACC-83 and SACC-LM cells without (migration assay, **Figure 3C**) or without Matrigel coating (invasive assay, **Figure 3D**).

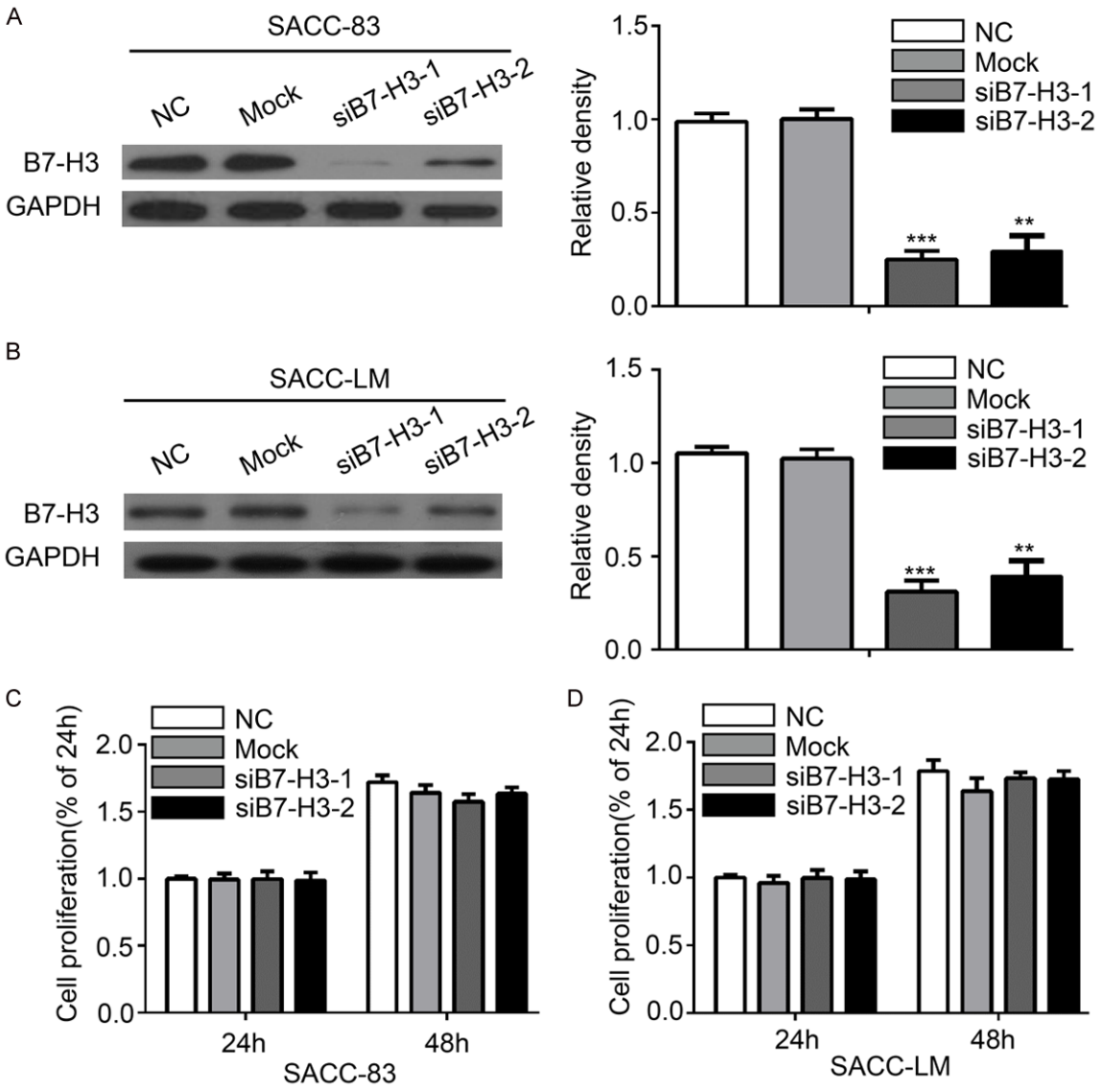


**Figure 2.** Knockdown of B7-H3 has no obvious effect on AdCC cell lines proliferation. A. Knockdown of B7-H3 by two different siRNA (siB7-H3-1 and siB7-H3-2) sequences in SACC-83 cell line, GAPDH served as a loading control; Relative intensive density were calculated by Image J, which represented mean of three independent experiments. NC, negative control; Mock, mock transfection; $^{**}P < 0.01$, $^{***}P < 0.001$; B. Knockdown of B7-H3 by two different siRNA sequences in SACC-LM cell line, GAPDH served as a loading control; Relative intensive density were calculated by Image J, which represented mean of three independent experiments. NC, negative control; Mock, mock transfection; $^{**}P < 0.01$, $^{***}P < 0.001$; C, D. B7-H3 siRNA interference had no obvious effect on SACC-83 and SACC-LM cell proliferation as indicated by MTT assay; Data represent mean ± SEM of three independent experiments.

*Knockdown of B7-H3 by siRNA suppressed the invasion and migration of AdCC cells by regulating the EMT via the JAK2/STAT3/Slug signaling pathway*

On the basis of the correlation between B7-H3 and the EMT marker (Slug), we hypothesized that B7-H3 influenced the EMT progression. siRNA was used to knock down B7-H3, and changes in EMT were determined by Western blotting of the putative EMT markers. The results showed that B7-H3 was involved in the EMT of AdCC cells. After knockdown of B7-H3, the expression of E-cadherin were upregulated, while N-cadherin, Slug, and vimentin were downregulated in the B7-H3 silenced groups compared with the negative control group in both the SACC-83 cells (**Figure 4A**) and the SACC-LM cells (**Figure 4B**). Furthermore, we detected the expression in the cell lines using immunofluorescence microscopy. Similar results were observed in SACC-83 cells (**Figure**

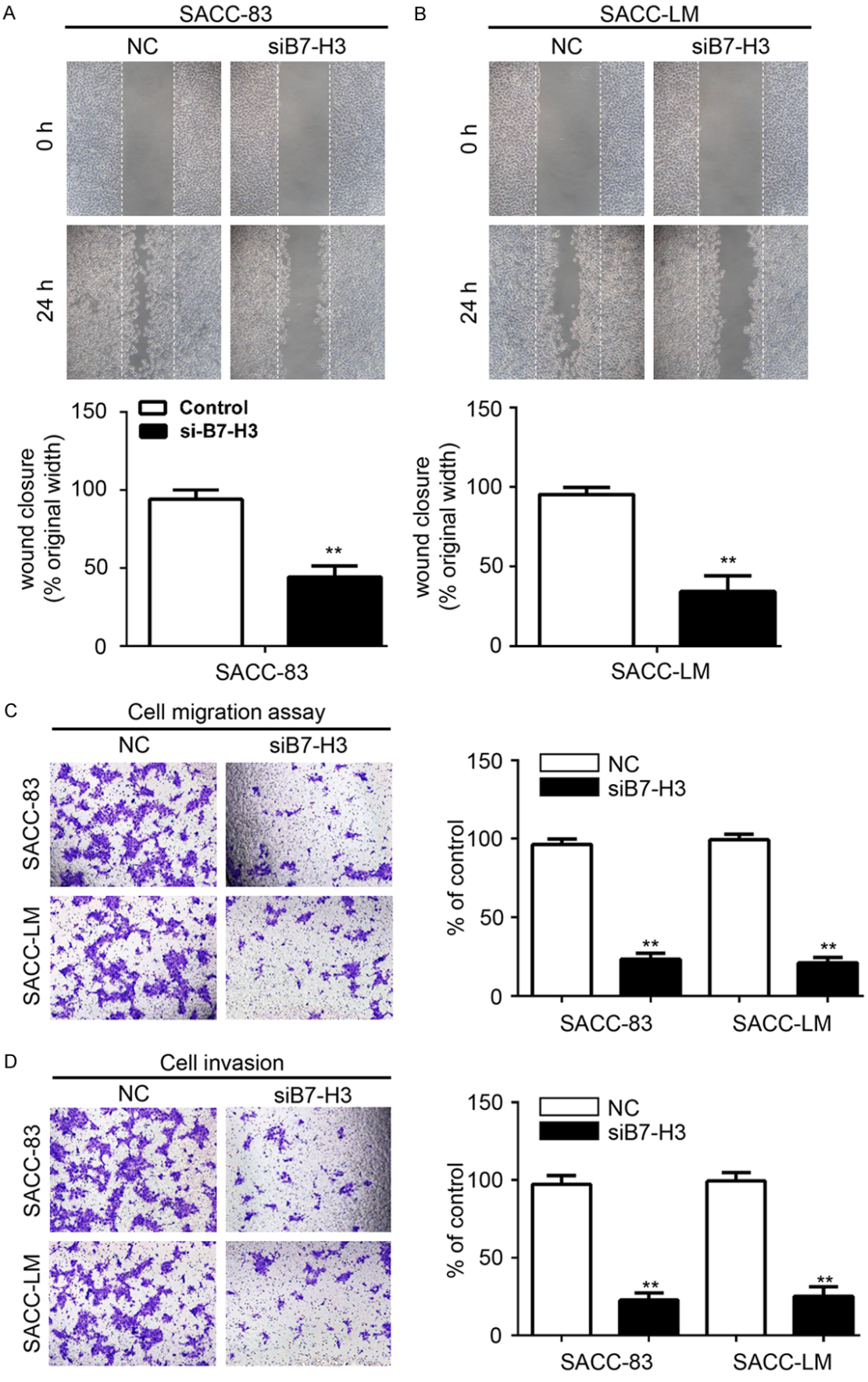
A
SACC-83
NC
siB7-H3
0 h
24 h
B
SACC-LM
NC
siB7-H3
0 h
24 h
Control
si-B7-H3
wound closure (% original width)
150
100
50
0
**
SACC-83
SACC-LM
C
Cell migration assay
NC
siB7-H3
SACC-83
SACC-LM
% of control
D
Cell invasion

**Figure 3.** Knockdown B7-H3 by RNA interference decrease AdCC cell lines migration and invasion. A and B. Wound healing assay showed knockdown of B7-H3 suppressed the cell mobility of SACC-83 and SACC-LM cell lines, and quantification of wound healing shows significant difference (Mean ± SEM; $^{**}P < 0.01$, student *t*-test with GraphPad Prism5.0); C. Migration assay using Transwell® chamber showed the decreased migration abilities of SACC-83 and SACC-LM after knockdown of B7-H3 compared with negative control group. D. Invasive assay by coating Matrigel® using Transwell® chamber showed the decreased invasive abilities of SACC-83 and SACC-LM after knockdown of B7-H3 compared with negative control group. The quantification of cell numbers with Image J "cell counter" module (Mean ± SEM; $^{**}P < 0.01$, student *t*-test with GraphPad Prism5.0).

**4C**) and SACC-LM cells (**Figure 4D**), with decreased vimentin and increased E-cadherin after knockdown of B7-H3. These results suggested that B7-H3 regulated the progression of EMT in AdCC.

The JAK2/STAT3 pathway is critical for cytokine and growth factor-mediated responses that regulate the EMT in fibrogenesis and cancer [20-22]. Because of the reported relationship between STAT3 and AdCC [17], and the role of STAT3 in cell motility and the EMT [22, 23], our study sought to directly examine the role of this pathway in B7-H3-induced EMT in AdCC cells. After transfection with B7-H3 siRNA, the phosphorylation of STAT3 and JAK2 was dramatically reduced in SACC-83 and SACC-LM cells, compared to that seen in the negative control group (**Figure 4E**, **4F**). However, the protein levels of JAK2 and STAT3 were not significantly changed (**Figure 4E**, **4F**). These results could explain, at least partially, the regulation of the EMT process by B7-H3, as being via the activation the JAK2/ STAT3/Slug signaling pathway.

## Discussion

In this study, we showed that the B7-H3 expression was significantly upregulated in human salivary AdCC, which was not associated with a subtype of salivary AdCC. On the basis of the AdCC tissue microarray results, we found that B7-H3 correlated with the levels of Slug and p-STAT3. Furthermore, *in vitro* functional studies suggested that knockdown of B7-H3 in AdCC cells decreased cell migration but had no effect on cell viability and apoptosis. Additionally, B7-H3 may have promoted the AdCC EMT via the JAK2/STAT3/Slug signaling pathway.

The remarkable clinical successes obtained from blocking the B7 superfamily of ligands, such as CTLA-4 and PD-1, have shown potential for cancer immunotherapy by inhibiting more recently discovered checkpoint ligands and receptors [24]. However, the tumor-associated antigen, B7-H3 has not only been attributed to tumor immunity but also may play a non-immunological role in cancer progression [4, 25-28]. Recent studies have reported that B7-H3 over-expression was observed in various cancers [8, 28, 29]. Consistent with these findings, immunohistochemical staining indicated that aberrant positive expression of B7-H3 in human salivary AdCC was observed in comparison with that of normal salivary glands, although B7-H3 expression was the same among cribriform, tubular, and solid subtypes of AdCC.

EMT is frequently observed at the invasive front of advanced tumors and significantly correlates with metastasis in tumor progression [11, 12]. EMT is a key event for cancerous cells to acquire the capability of migration and invasion [30, 31]. These processes are tightly temporally and spatially regulated by the expression and activation of many signal molecules [32-34]. A recent report suggested that Slug is the key molecule regulating EMT programming in cancer [35]. We have previously reported that Slug-mediated EMT plays an important role in the process of metastasis [16]. In addition, the replacement of E-cadherin by N-cadherin during the EMT promoted the invasiveness and metastasis of tumor cells [36]. When we determined the variation of EMT markers, the results showed up-regulation of an epithelial marker, whereas the down-regulation of the mesenchymal markers N-cadherin and Slug were as predicted.

Our previous study demonstrated that targeting STAT3 reduced the migration and invasion of AdCC cells [17]. In present study, we found that the expression of B7-H3 was positively associated with p-STAT3 level. We also observed that p-JAK2 and p-STAT3 were down-regulated after the knockdown of B7-H3. In agreement with previous findings, B7-H3 regulated JAK2/STAT3 signaling in colorectal cancer and hepatocellu-

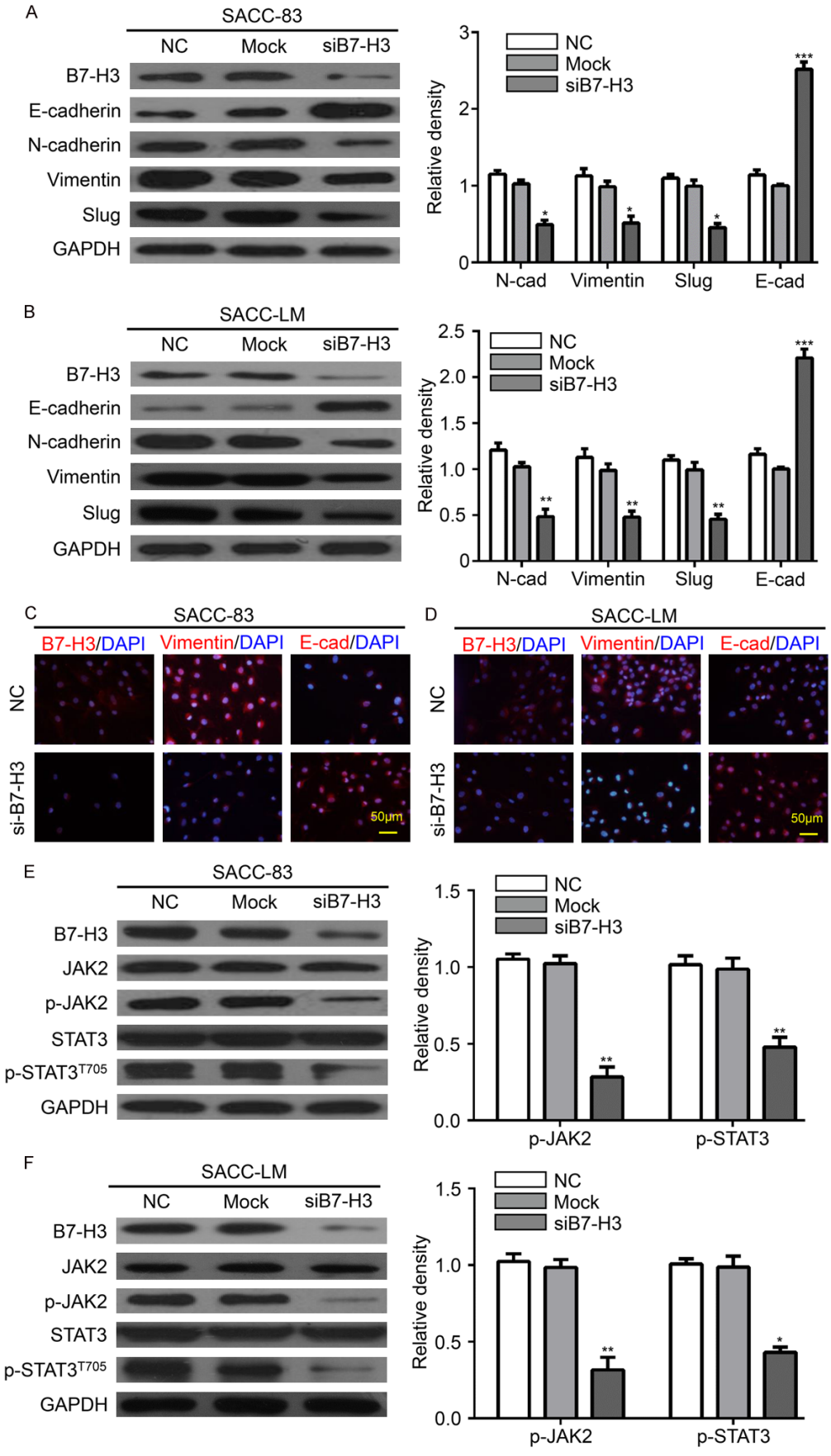
A
SACC-83
NC
Mock
siB7-H3
B7-H3
E-cadherin
N-cadherin
Vimentin
Slug
GAPDH
Relative density
N-cad
Vimentin
Slug
E-cad
B
SACC-LM
C
SACC-83
B7-H3/DAPI
Vimentin/DAPI
E-cad/DAPI
si-B7-H3
50μm
D
SACC-LM
E
JAK2
p-JAK2
STAT3
p-STAT3T705
p-JAK2
p-STAT3
F

**Figure 4.** Knockdown of B7-H3 suppresses the EMT via JAK2/STAT3/Slug signaling. A, B. Knockdown of B7-H3 using siRNA decreased the EMT in SACC-83 and SACC-LM cell lines, as indicated by increased E-cadherin and decreased N-cadherin, Vimentin and Slug by Western blotting. GAPDH was used as a loading control. The quantification of blotting are presented as the means ± SEM by 3 different experiments. One-way ANOVA with post-Tukey analysis was performed using GraphPad Prism5. $*P < 0.05$; $**P < 0.01$; $***P < 0.001$ versus the negative control group (NC, n = 3); Mock, mock transfection. C, D. The representative immunofluorescence of B7-H3, E-cadherin and Vimentin of B7-H3 knockdown in SACC-83 and SACC-LM cell lines compared with negative control (NC) and mock counterpart (Scale bars = 50 μm); E, F. Knockdown B7-H3 decreased JAK2/p-STAT3 signaling in SACC-83 and SACC-LM cell lines as indicated by the JAK2, p-JAK2, STAT3 and p-STAT3$^{T705}$ Western blotting. GAPDH was used as a loading control. The values are presented as the means ± SEM. One-way ANOVA with post-Dunnett analysis was performed using GraphPad Prism5. $*P < 0.05$, $**P < 0.01$; versus the negative control group (n = 3) Mock, mock transfection.

lar carcinoma [32, 37]. Based on these results and those from previous reports, we confirmed the close relationship between B7-H3 and JAK2/STAT3 signaling.

In conclusion, this study demonstrated that B7-H3 was up-regulated in the salivary AdCC. B7-H3 knockdown inhibited the EMT process, and the JAK2/STAT3 signaling pathway played an important role in this process. These findings supported the possibility of using B7-H3 as a target for anti-metastatic therapy in salivary AdCC.

## Acknowledgements

This work was supported by National Natural Science Foundation of China (81672668, 81672667, 81472528, 81472529, 81272963, 81272964). Z.J.S. was supported by program for new century excellent talents in university, Ministry of Education of China (NCET-13-0439). T.F.W. was supported by the Fundamental Research Funds for the Central Universities (No. 2042015kf0075).

## Disclosure of conflict of interest

None.

**Address correspondence to:** Zhi-Jun Sun, Department of Oral Maxillofacial-Head Neck Oncology, School and Hospital of Stomatology, Wuhan University, 237 Luoyu Road, Wuhan, China. Tel: +86-27-87686108; E-mail: zhijundejia@163.com

## References

[1] Laurie SA, Ho AL, Fury MG, Sherman E and Pfister DG. Systemic therapy in the management of metastatic or locally recurrent adenoid cystic carcinoma of the salivary glands: a systematic review. Lancet Oncol 2011; 12: 815-824.

[2] Coca-Pelaz A, Rodrigo JP, Bradley PJ, Vander Poorten V, Triantafyllou A, Hunt JL, Strojan P, Rinaldo A, Haigentz M Jr, Takes RP, Mondin V, Teymoortash A, Thompson LD and Ferlito A. Adenoid cystic carcinoma of the head and neck--an update. Oral Oncol 2015; 51: 652-661.

[3] Gao M, Hao Y, Huang MX, Ma DQ, Luo HY, Gao Y, Peng X and Yu GY. Clinicopathological study of distant metastases of salivary adenoid cystic carcinoma. Int J Oral Maxillofac Surg 2013; 42: 923-928.

[4] Chapoval AI, Ni J, Lau JS, Wilcox RA, Flies DB, Liu D, Dong H, Sica GL, Zhu G, Tamada K and Chen L. B7-H3: a costimulatory molecule for T cell activation and IFN-gamma production. Nat Immunol 2001; 2: 269-274.

[5] Leitner J, Klauser C, Pickl WF, Stockl J, Majdic O, Bardet AF, Kreil DP, Dong C, Yamazaki T, Zlabinger G, Pfistershammer K and Steinberger P. B7-H3 is a potent inhibitor of human T-cell activation: no evidence for B7-H3 and TREML2 interaction. Eur J Immunol 2009; 39: 1754-1764.

[6] Wang L, Kang FB and Shan BE. B7-H3-mediated tumor immunology: friend or foe? Int J Cancer 2014; 134: 2764-2771.

[7] Wang J, Chong KK, Nakamura Y, Nguyen L, Huang SK, Kuo C, Zhang W, Yu H, Morton DL and Hoon DS. B7-H3 associated with tumor progression and epigenetic regulatory activity in cutaneous melanoma. J Invest Dermatol 2013; 133: 2050-2058.

[8] Chen L, Chen J, Xu B, Wang Q, Zhou W, Zhang G, Sun J, Shi L, Pei H, Wu C and Jiang J. B7-H3 expression associates with tumor invasion and patient's poor survival in human esophageal cancer. Am J Transl Res 2015; 7: 2646-2660.

[9] Thiery JP. Epithelial-mesenchymal transitions in tumour progression. Nat Rev Cancer 2002; 2: 442-454.

[10] Zhang H, Sun JD, Yan LJ and Zhao XP. PDGF-D/PDGFRbeta promotes tongue squamous carcinoma cell (TSCC) progression via activating p38/AKT/ERK/EMT signal pathway. Biochem Biophys Res Commun 2016; 478: 845-851.

[11] Ye LY, Chen W, Bai XL, Xu XY, Zhang Q, Xia XF, Sun X, Li GG, Hu QD, Fu QH and Liang TB. Hypoxia-induced epithelial-to-mesenchymal transition in hepatocellular carcinoma induces an immunosuppressive tumor microenvironment to promote metastasis. Cancer Res 2016; 76: 818-830.
[12] Brabletz T. To differentiate or not--routes towards metastasis. Nat Rev Cancer 2012; 12: 425-436.
[13] Kim J, Kim TY, Lee MS, Mun JY, Ihm C and Kim SA. Exosome cargo reflects TGF-beta1-mediated epithelial-to-mesenchymal transition (EMT) status in A549 human lung adenocarcinoma cells. Biochem Biophys Res Commun 2016; 478: 643-648.
[14] Yu GT, Bu LL, Zhao YY, Liu B, Zhang WF, Zhao YF, Zhang L and Sun ZJ. Inhibition of mTOR reduce Stat3 and PAI related angiogenesis in salivary gland adenoid cystic carcinoma. Am J Cancer Res 2014; 4: 764-775.
[15] Fan TF, Bu LL, Wang WM, Ma SR, Liu JF, Deng WW, Mao L, Yu GT, Huang CF, Liu B, Zhang WF and Sun ZJ. Tumor growth suppression by inhibiting both autophagy and STAT3 signaling in HNSCC. Oncotarget 2015; 6: 43581-43593.
[16] Zhao ZL, Ma SR, Wang WM, Huang CF, Yu GT, Wu TF, Bu LL, Wang YF, Zhao YF, Zhang WF and Sun ZJ. Notch signaling induces epithelial-mesenchymal transition to promote invasion and metastasis in adenoid cystic carcinoma. Am J Transl Res 2015; 7: 162-174.
[17] Bu LL, Deng WW, Huang CF, Liu B, Zhang WF and Sun ZJ. Inhibition of STAT3 reduces proliferation and invasion in salivary gland adenoid cystic carcinoma. Am J Cancer Res 2015; 5: 1751-1761.
[18] Fan TF, Wu TF, Bu LL, Ma SR, Li YC, Mao L, Sun ZJ and Zhang WF. Dihydromyricetin promotes autophagy and apoptosis through ROS-STAT3 signaling in head and neck squamous cell carcinoma. Oncotarget 2016; 7: 59691-59703.
[19] Sun ZJ, Chen G, Zhang W, Hu X, Huang CF, Wang YF, Jia J and Zhao YF. Mammalian target of rapamycin pathway promotes tumor-induced angiogenesis in adenoid cystic carcinoma: its suppression by isoliquiritigenin through dual activation of c-Jun NH2-terminal kinase and inhibition of extracellular signal-regulated kinase. J Pharmacol Exp Ther 2010; 334: 500-512.
[20] Chen J, Lan T, Zhang W, Dong L, Kang N, Zhang S, Fu M, Liu B, Liu K and Zhan Q. Feed-forward reciprocal activation of pafr and STAT3 regulates epithelial-mesenchymal transition in non-small cell lung cancer. Cancer Res 2015; 75: 4198-4210.
[21] Zhao D, Besser AH, Wander SA, Sun J, Zhou W, Wang B, Ince T, Durante MA, Guo W, Mills G, Theodorescu D and Slingerland J. Cytoplasmic p27 promotes epithelial-mesenchymal transition and tumor metastasis via STAT3-mediated Twist1 upregulation. Oncogene 2015; 34: 5447-5459.
[22] Kim MS, Lee WS, Jeong J, Kim SJ and Jin W. Induction of metastatic potential by TrkB via activation of IL6/JAK2/STAT3 and PI3K/AKT signaling in breast cancer. Oncotarget 2015; 6: 40158-40171.
[23] Colomiere M, Ward AC, Riley C, Trenerry MK, Cameron-Smith D, Findlay J, Ackland L and Ahmed N. Cross talk of signals between EGFR and IL-6R through JAK2/STAT3 mediate epithelial-mesenchymal transition in ovarian carcinomas. Br J Cancer 2009; 100: 134-144.
[24] Woods K and Cebon J. Tumor-specific T-cell help is associated with improved survival in melanoma. Clin Cancer Res 2013; 19: 4021-4023.
[25] Zang X, Thompson RH, Al-Ahmadie HA, Serio AM, Reuter VE, Eastham JA, Scardino PT, Sharma P and Allison JP. B7-H3 and B7x are highly expressed in human prostate cancer and associated with disease spread and poor outcome. Proc Natl Acad Sci U S A 2007; 104: 19458-19463.
[26] Vigdorovich V, Ramagopal UA, Lazar-Molnar E, Sylvestre E, Lee JS, Hofmeyer KA, Zang X, Nathenson SG and Almo SC. Structure and T cell inhibition properties of B7 family member, B7-H3. Structure 2013; 21: 707-717.
[27] Suh WK, Gajewska BU, Okada H, Gronski MA, Bertram EM, Dawicki W, Duncan GS, Bukczynski J, Plyte S, Elia A, Wakeham A, Itie A, Chung S, Da Costa J, Arya S, Horan T, Campbell P, Gaida K, Ohashi PS, Watts TH, Yoshinaga SK, Bray MR, Jordana M and Mak TW. The B7 family member B7-H3 preferentially down-regulates T helper type 1-mediated immune responses. Nat Immunol 2003; 4: 899-906.
[28] Chen JT, Chen CH, Ku KL, Hsiao M, Chiang CP, Hsu TL, Chen MH and Wong CH. Glycoprotein B7-H3 overexpression and aberrant glycosylation in oral cancer and immune response. Proc Natl Acad Sci U S A 2015; 112: 13057-13062.
[29] Zhang SS, Tang J, Yu SY, Ma LI, Wang F, Xie SL, Jin L and Yang HY. Expression levels of B7-H3 and TLT-2 in human oral squamous cell carcinoma. Oncol Lett 2015; 10: 1063-1068.
[30] Lamouille S, Xu J and Derynck R. Molecular mechanisms of epithelial-mesenchymal transition. Nat Rev Mol Cell Biol 2014; 15: 178-196.
[31] De Craene B and Berx G. Regulatory networks defining EMT during cancer initiation and progression. Nat Rev Cancer 2013; 13: 97-110.
[32] Kang FB, Wang L, Jia HC, Li D, Li HJ, Zhang YG and Sun DX. B7-H3 promotes aggression and

invasion of hepatocellular carcinoma by targeting epithelial-to-mesenchymal transition via JAK2/STAT3/Slug signaling pathway. Cancer Cell Int 2015; 15: 45.

[33] Yadav A, Kumar B, Datta J, Teknos TN and Kumar P. IL-6 promotes head and neck tumor metastasis by inducing epithelial-mesenchymal transition via the JAK-STAT3-SNAIL signaling pathway. Mol Cancer Res 2011; 9: 1658-1667.

[34] Tam WL and Weinberg RA. The epigenetics of epithelial-mesenchymal plasticity in cancer. Nat Med 2013; 19: 1438-1449.

[35] Guo W, Keckesova Z, Donaher JL, Shibue T, Tischler V, Reinhardt F, Itzkovitz S, Noske A, Zurrer-Hardi U, Bell G, Tam WL, Mani SA, van Oudenaarden A and Weinberg RA. Slug and Sox9 cooperatively determine the mammary stem cell state. Cell 2012; 148: 1015-1028.

[36] Guarino M. Epithelial-mesenchymal transition and tumour invasion. Int J Biochem Cell Biol 2007; 39: 2153-2160.

[37] Zhang T, Jiang B, Zou ST, Liu F and Hua D. Overexpression of B7-H3 augments anti-apoptosis of colorectal cancer cells by Jak2-STAT3. World J Gastroenterol 2015; 21: 1804-1813.